ICAS 2016
30th Congress of the International Council of the Aeronautical Sciences
DCC, Daejeon, Korea ; September 25-30, 2016

ELASTO-STATIC AND MODAL MODELING OF FLEXIBLE WINGS CARRYING MULTIPLE EXTERNAL STORES

E. M. Amato[1], C. Polsinelli[2], E. Cestino[3], G. Frulla[4], R. Carrese,[5] P. Marzocca[6]

[1,2,3,4] **Dept Mechanical and Aerospace Eng. (DIMEAS), Politecnico di Torino, Turin, Italy**
[5,6] **School of Engineering, Aerospace Engineering and Aviation, RMIT University, Melbourne, Australia**
Corresponding author e-mail: *pier.marzocca@rmit.edu.au*

Keywords: *Flexible wing, stores, elasto-static and modal modeling*

Abstract

The design of highly flexible aircraft involves several critical phenomena which are not considered in traditional aircraft design. Large structural deflections under nominal loads and flight conditions, point out that a linear structural model is often inadequate in the accurate flutter prediction. In place of a linear Euler-Bernoulli theory, usually sufficient in the evaluation of natural frequencies of slender structures when deflections are lower than transversal dimensions, a nonlinear analysis is required as there is strong dependency between natural frequencies and beam deflections which could lead to flutter instability at lower flight speeds. The model complexities increase when one or more stores are placed under the wing. In this study numerical and experimental investigations are carried out to better understand the nonlinear behaviour of highly flexible wings with external stores positioned at selected spanwise, chordwise, and flapwise stations, when both geometrical and aerodynamic nonlinearities are not negligible. Good correlation between numerical and experimental investigations was found, showing strong edge and torsion frequencies and associated mode shapes dependency on the initial deformation.

1. Introduction

Lightweight and flexible *high-altitude long endurance (HALE)* wings exhibits uncommon aeroelastic behaviour. Since aeroelastic instabilities constrain the flight envelope of HALE aircraft and have a fundamental role in their design process, modelling and aeroelastic characterization has to be done with particular care. Specifically, system modelling should account for structural and aerodynamic nonlinearities which often dominate their behaviour. Even moderate deflections cause nonlinear stiffening that modifies the wing aeroelastic dynamics. As a result, it is necessary to carry out flutter analysis considering the large deflection state as a reference condition. Moreover when stores are placed under the wing, the wing dynamics change with significant reduction of the flutter speed. The presence of multiple stores modifies both mode-shapes as well as natural frequencies. As inertial effects changes the torsional frequencies, coupling between flap and edgewise bending and between torsional and edgewise bending frequencies are triggered.
Consequently, the understanding the correlation between the change of dynamics behaviour and the flutter speed variation is of critical importance in order to guarantee the system reliability as well as the airworthiness requirements. Several archival papers deal with the aeroelasticity of slender wings. Dowell [5] collects several studies pertinent to nonlinear aeroelasticity in a comprehensive review. Patil and Hodges [4] pointed out a great influence of geometrical nonlinearities on the dynamic behaviour. A large spanwise deflection and variation of structural frequencies was shown by

inducing a static deformation by mean of a static force applied at the tip. The strong coupling between the edgewise and torsional frequencies was due to the beam static deflection. Generally speaking, torsional and edge frequency were also decreasing and yielded a reduction in the flutter speed proportional to the static tip displacement. In [6] the authors have shown the dependence between flutter speed, LCO and stores position. They investigated the effect of the numbers of stores, mass and moment of inertia in different tested configurations. The results have shown a great influence with respect to the stores position in spanwise and chordwise directions. A typical HALE configuration with high aspect ratios was also considered in [3] and the discrepancy between nonlinear and linear flutter predictions was highlighted. It was shown that the flutter behaviour could be improved if the chord-wise stiffness is increased, while the store placed under the wing at the tip could potentially decrease the flutter speed up to 83% of the clean wing configuration. Patil and Hodges [7] analyzed different types of geometrical nonlinearities with respect to aeroelastic behaviour of high-aspect-ratio wings. They have shown that the difference, between the air-loads calculated by means of a nonplanar wing geometry theory as compared with the same loads achieved with planar theory, is negligible. Instead, the dynamics behaviour of the wing undergoing large deflections exhibits a significant change, even more than 50% reduction on the prediction of the flutter speed. The wing model presented in this paper is taken from [1] and [2]. It has a wood spar with several ABS non-structural aerodynamically shaped parts. All wing components with the exception of the spar are produced with additive manufacturing processes. A nonlinear theory is applied for the investigation of static and dynamics performance of such a wing under different load conditions yielding deflections higher than 10% of the wing spanwise length.

2. Cantilever Beam Analysis

Several cantilever beam configurations, to understand the changes in natural frequencies when the structure is under large deflections, was carried out first. This analysis was also a necessary one to select an appropriate geometrical configuration which would emphasize the effect of the geometrical nonlinearities. The selected beam properties are as follows: Length: *L=500 mm*; Material: Aluminum; Density: *2710 kg/m*^{3}; Young Module: *E=73 GPa*; Yield Stress: σ*=345 MPa.* During the numerical analysis the yield strength limit was not exceeded, as to avoid to produce others nonlinearity caused by nonlinear material behaviour. The nonlinear behavior was induced by increasing the magnitude of the tip force which in turn increased the flap displacement. Gravity force was also included into the loads. As expected, these preliminary investigations showed that no changes in the natural frequencies occurred for small deflections and the linear analysis was sufficiently accurate, while the frequencies would change for larger beam deformation and could be captured only by performing a nonlinear analysis. Numerical model, made with nonlinear FEM software ABAQUS® by SIMULIA, was verified by using the Euler-Bernoulli linear theory.

2.1. Numerical Investigation

The reference body axis are x in the chord-wise direction, y perpendicular to chord-wise direction and z in the span-wise direction. The different cross-sections analyzed have the following shapes: a) Rectangular (R), b) I and c) U shape. Dimensions and shapes dimensions are reported in Tables 1 and 3 and Fig. . 1, respectively. Each section is represented by using two parameters [1]: $\Gamma = EI_y/EI_x$ and $\vartheta = GJ_t/EI_x$. Figure 2 shows the percent error between linear and nonlinear theory when the large displacement is taken into account. With a tip deflection of 20% (100 mm) the linear/nonlinear error is about 3÷4% while reaches 15% for a tip deflection of 40%. The nonlinear analysis provides more accurate predictions as the applied load and resulting deformation increase.

Rectangular sections

The first transversal geometry taken into account is a simple rectangular cross-section beam (R-type) with 20mm base and several

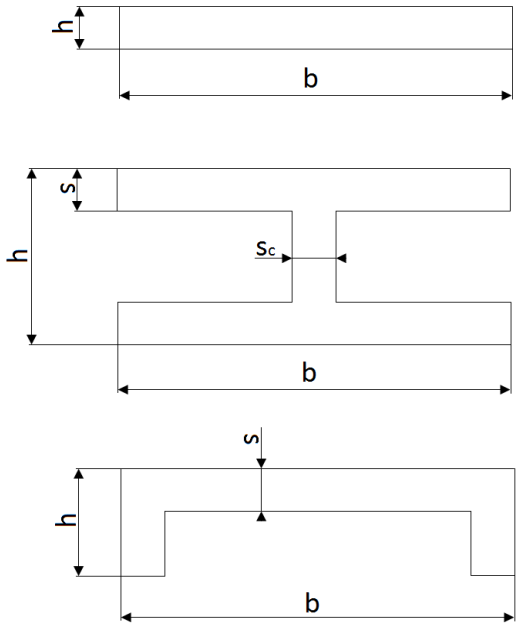

Fig. 1 Section types

height values as reported in Table 1. In Table 2 the theoretical e numerical natural frequencies are reported. Figures 3 through 5 display the natural frequencies obtained through numerical investigations performed using both linear and nonlinear analysis. Edge and torsion frequencies demonstrate an important coupling with deflections: a tip displacement of 38% of the length introduces a reduction of 70% in the first edge frequency for section thickness of 1mm.

I and U Sections

When considering the I and U cross-sections, the most influenced modes are also edge and torsion. By comparing the nonlinear effects on

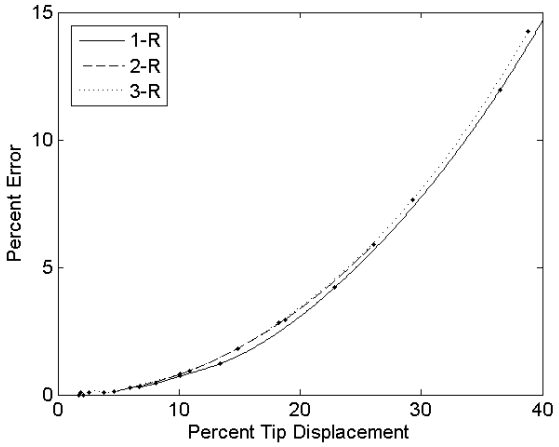

Fig. 2 Lin. vs N-Lin. tip displacement percent error.

the natural frequencies with the geometrical parameters, it can be concluded that such behavior depends on the cross-section geometry as well as the two parameters Γ and ϑ. It means that with the same geometrical parameters but different cross-section, the nonlinear beam behavior might be not the same.

Additionally, the investigation also shows that for the I-type section and for increasing Γ, larger variations in natural frequencies are displayed. This does not occur for U-type cross sections, and it is probably due to ϑ, which is significantly different between the two considered sections.

Notwithstanding, these initial investigations clearly show the importance of taking large deflection nonlinearities into account. Figure 6 through 8 show the numerical results.

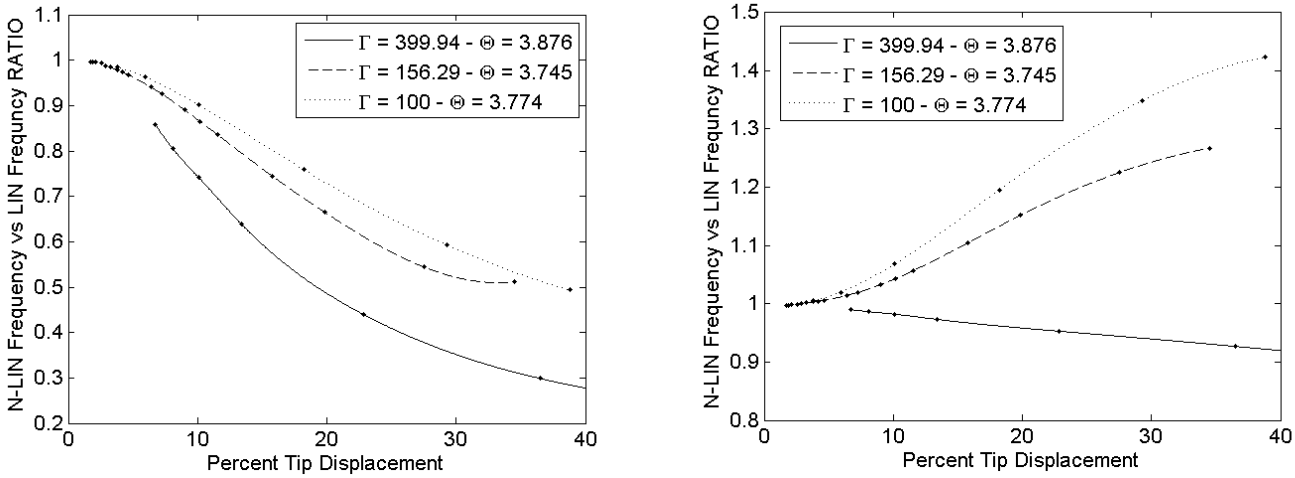

Fig. 3 1st and 2nd nonlinear Edge frequencies, variation in % with respect to the linear case. R typology.

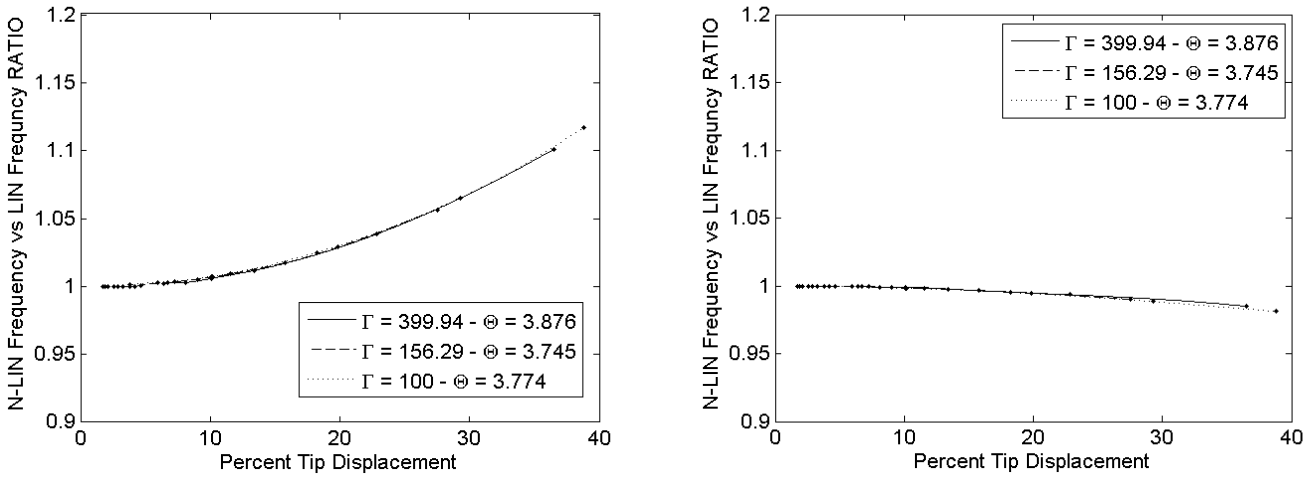

Fig. 4 1st and 2nd nonlinear Bending frequencies, variation in % with respect to the linear case. R typology.

Type	Thickness[mm]	Γ	Θ
1-R	1	399.64	3.87
2-R	1.6	156.29	3.74
3-R	2	100.00	3.77

Tab. 1 Rectangular cross-section with 20 mm base, geometrical parameters

	1-R		2-R		3-R	
	Num	Th	Num	Th	Num	Th
bdg1	3.36	3.36	5.38	5.22	6.73	6.72
bdg2	21.08	21.06	33.72	32.72	42.15	42.11
edg1	66.94	67.20	66.20	67.20	66.94	67.20
edg2	416.41	421.12	416.722	412.12	416.41	421.12
trs1	158.18	156.68	251.27	247.75	309.73	307.08

Tab. 2 Rectangular cross-section: numerical and theoretical natural frequencies

2.2 Experimental campaign

An experimental campaign was developed in order to investigate and validate previous numerical results.
The beam tip deflection was induced by changing the length of the test model.
Other methods were explored but not implemented; a tip mass used to induce a tip displacement, would have changed the boundary condition at the tip and consequently the mode shapes and frequencies, the use of a distributed mass, would have been quite difficult to identify. From the Euler-Bernoulli linear beam theory, which discards the rotatory

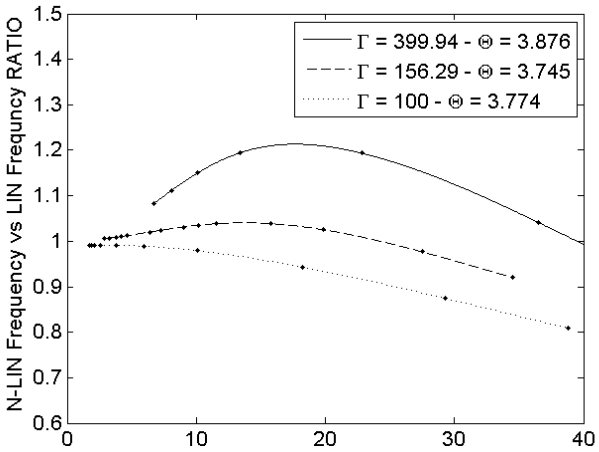

Fig. 5 1st Torsion frequencies, variation in % with respect to the linear case. R typology.

Type	b	H	s	s_c	Γ	Θ
1-I	20	5	1	1	8.05	0.084
2-I	10	5	1	1	1.99	0.086
3-I	10	5	1.5	2	2.51	0.261
1-U	7	4	1.5	n/a	4.32	0.491
2-U	10	4	1.6	n/a	0.97	0.064

Tab. 3 I and U cross-section geometrical parameters: b, h, s and s_c in mm

inertia considering a uniform distribution of weight (μ), the natural frequencies follow the relationship $f_n = C_m \cdot \beta_n^2$ where C_m is function of the material and $\beta_n^4 = \mu \cdot \omega_n^2 / D$. Remembering that the free vibration equation can be cast as $\psi_{,xxxx} - \beta^4 \cdot \psi = 0$, it is possible to obtain the eigenvalues of the system, namely $\lambda_i = (\beta \cdot L)_i$, and a frequency index,

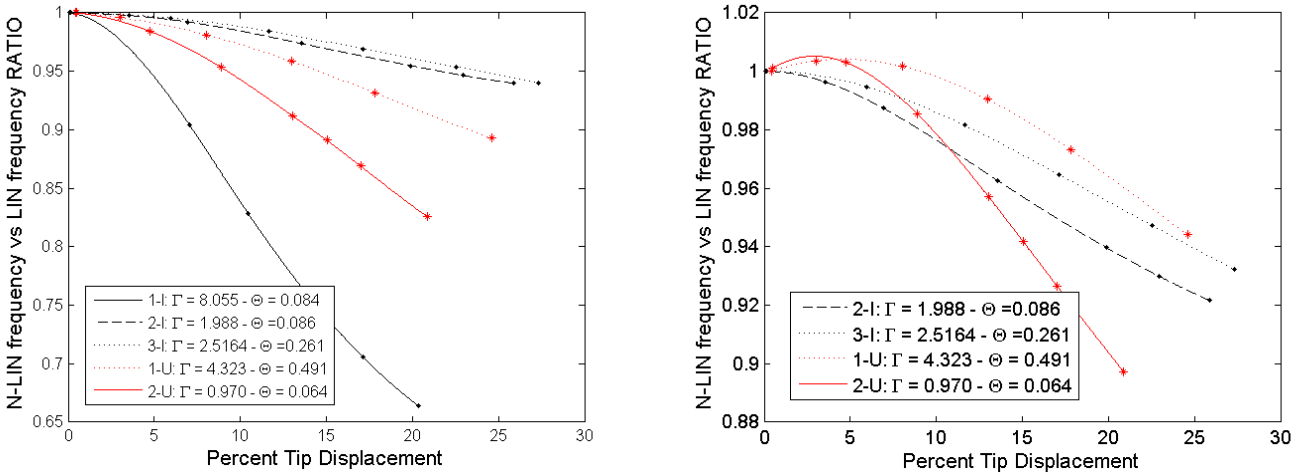

Fig. 6 1st and 2nd non-linear Edge frequencies, variation in % with respect to the linear case. I and U typology.

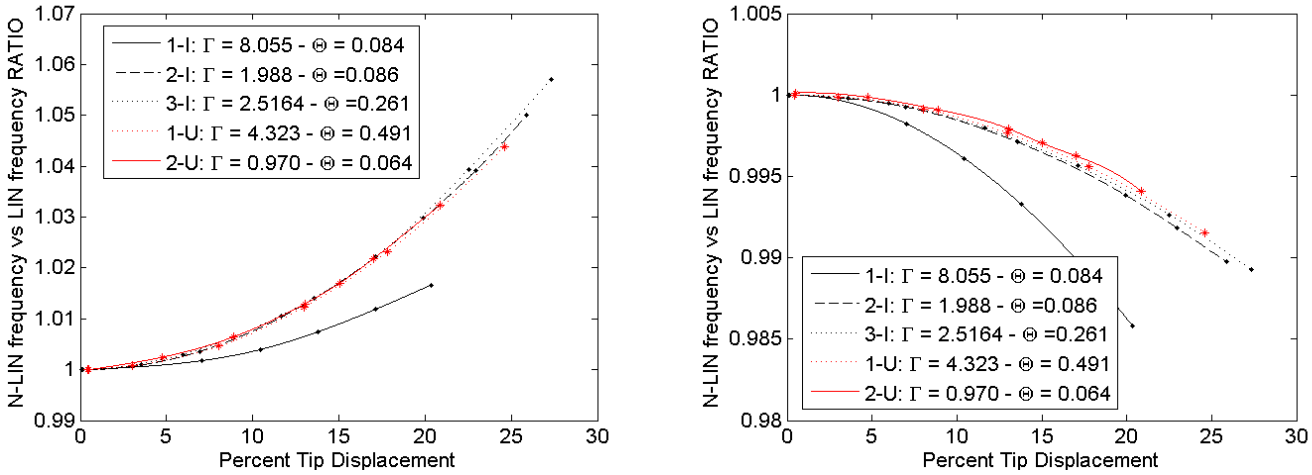

Fig. 7 1st and 2nd nonlinear Bending frequencies, variation in % with respect to the linear case. I and U typology.

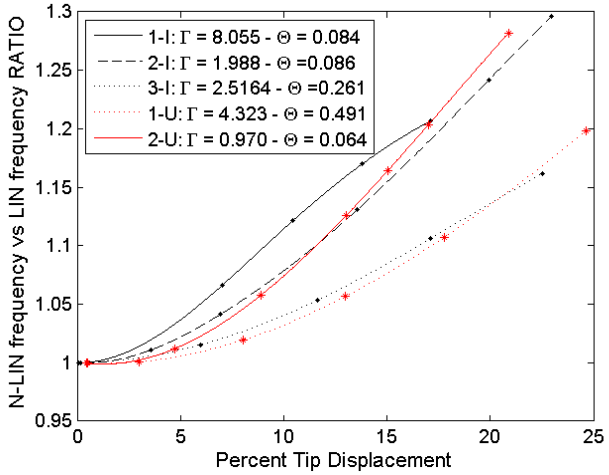

Fig. 8 1st Torsion frequencies, percent variation respect linear case. I and U typology.

independent from the beam length. For the transverse and edge vibrations these are: $\tau n = fn \cdot L2$ while for the torsion frequencies are: $\tau tn = ftn \cdot L$. It is worth noting that the dynamic analysis of a beam with increasing length can give the same linear τ parameter, while the nonlinear counterpart changes. The tested 20x1.6mm rectangular beam was analysed by means of a laser scanning vibrometer PSV-400 by Polytec, while a shaker was used to apply a point source white noise. By using the laser scanning vibrometer the time-histories of the deflections were collected at a sufficient number of locations to build the mode shape and find the first natural frequencies. With respect to the experimental linear analysis, the beam was placed in vertical to prevent the deformation, approximating the linear behaviour, as illustrated in Fig. 9. Two excitation methods were used: a) the shaker was positioned in firm contact with the beam near the clamp (root excitation); b) the beam was clamped on the shaker (base excitation).

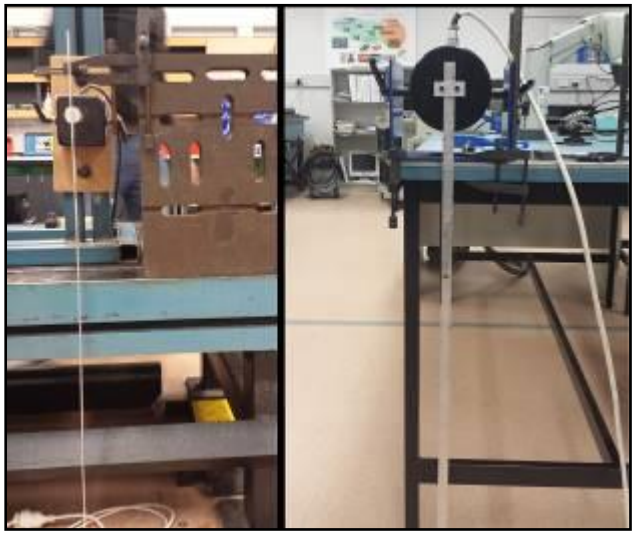

Fig. 9 Experimental setup

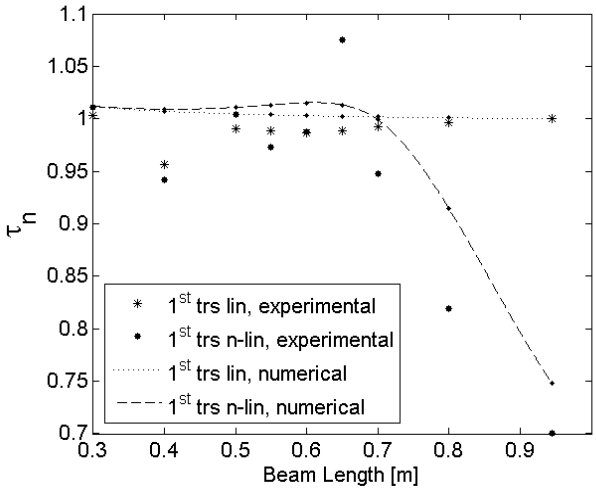

Fig. 10 Normalize τ_{tn} parameter for torsion data.

The two analyses lead at the same results, for this reason they will be considered without any distinction. A preliminary numerical analysis was done for each experimental configuration in order to assess the model accuracy. The comparison between numerical and experimental analysis is reported in the subsequent figures. Numerical predictions in Fig. 10 through 12, confirm that τ values at different length are always constant when the assumption of linearity holds valid (all results were normalized with the linear values at length 950mm, both numerical and experimental). The nonlinear torsion analysis highlights an increase in the frequency ratio for shorter beams, while an opposite trend is noticeable for longer beams as the assumption of linearity breaks down. This nonlinear behavior should be examined more thoroughly.

Clearly the torsional frequency is influenced by the beam length. Considering a cantilever configuration mounted vertically to reduce gravity effect, and comparing the difference of value between linear and nonlinear analyses, larger discrepancies are evident for longer beams.

Table 4 presents the values of tip displacement for each beam length configuration. When considering the nonlinear flapwise bending, the difference between the two analyses is negligible, less than 5% for the most influenced frequencies. Contrarily, the edge frequencies display large difference between linear and nonlinear values. The 1st edge frequency dropped by a factor of 35 and the 2nd increased by 55 when compared with a linear analysis.

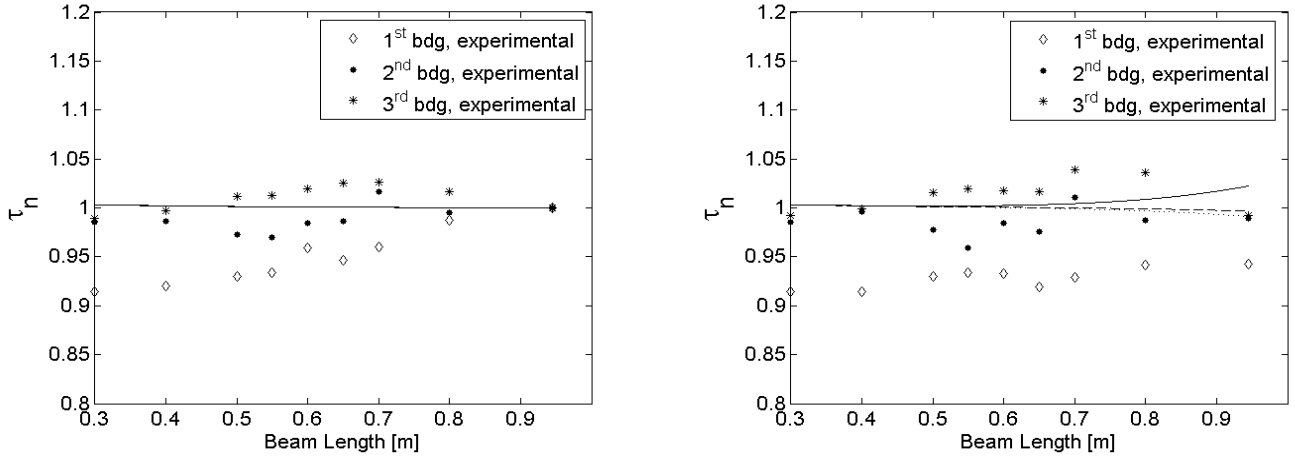

Fig. 11 Normalized τ_n parameter for Bending linear and non-linear data.

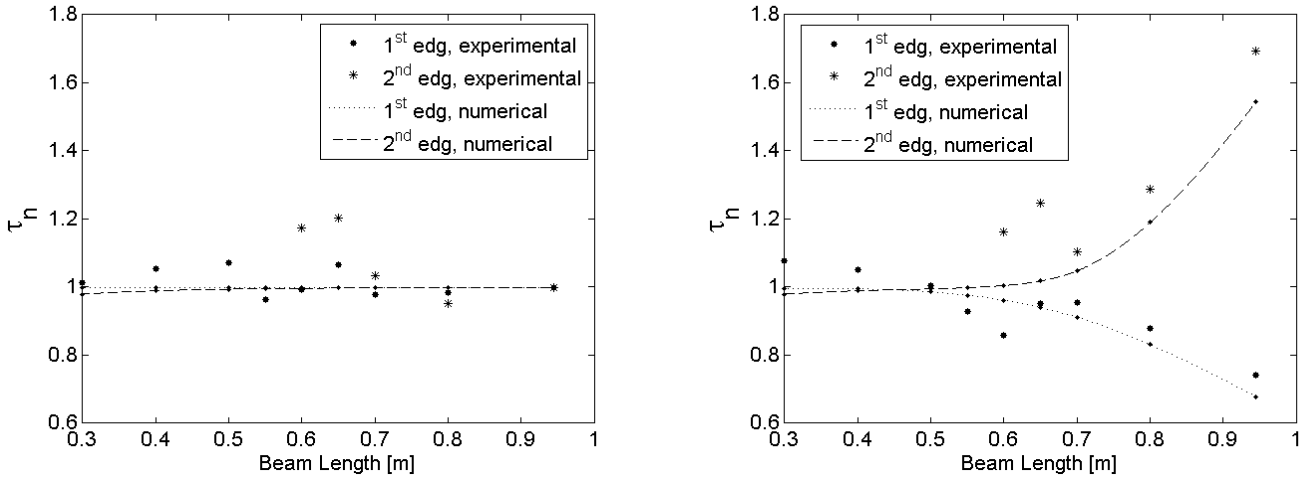

Fig. 12 Normalized τ_n parameter for Edge linear and non-linear data.

Good correlation is shown between numerical and experimental data. The minor discrepancy can be attributed to manufacturing imperfections, material property estimations, the position of the beam and the root clamp setup. Because of such small discrepancy in the bending mode there is only a very small visible difference between the linear and nonlinear analysis. Indeed, when comparing experimental and numerical predictions for the 1st bending frequency the error is less than 8%. However, it is worth noting that the 1st nonlinear bending frequency increases with the length of the beam in the numerical analysis, but it decreases in the experimental campaign.

L [mm]	Tip-Displ. [mm]	Tip-Displ. %
300	1.71	0.57
400	5.40	1.35
500	13.20	2.64
550	19.33	3.51
600	27.53	4.59
650	37.69	5.80
700	55.78	7.97
800	94.74	11.84
950	181.80	19.14

Tab. 4 Tip displacement for each beam length

However, the frequency values, for each length, are within 1.4 Hz and 14.5 Hz for the longest beam tested, with has a length of 950 mm; the 1st bending frequency computed using a 1.56 Hz in the linear analysis and 1.47 Hz in the nonlinear analysis, just a 5.77% error (0.09 Hz). These findings demonstrate that there are no significant changes between two experimental linear and nonlinear analyses which confirm the small sensitivity of the bending mode with respect to the tip displacement.

Very good correlations between experiments and numerical results are also shown for all the other considered frequencies and modes. It is also worth reporting that there is a notable difference at a beam length station between 600÷700 mm from the root.

Several analyses have been repeated to confirm the results and the variance is attributed to material or manufacturing imperfection in the aluminum beam.

Fig. 13 Assembled Wing.

I_{11}	$2.012 \cdot 10^{-7}$ kg/m^2
I_{22}	$5.74 \cdot 10^{-6}$ kg/m^2
I_{33}	$5.84 \cdot 10^{-6}$ kg/m^2
Material	Titanium
Density	4500 kg/m^3
Weight(1Pz)	0.014 kg

Tab. 5 Stores properties

POS	X(mm)	Y (mm)	Z(mm)
1	0	-7.59	125
2	0	-7.59	250
3	0	-7.59	375
4	0	-7.59	500
4.1	-9.09	-7.59	500
4.2	6.66	-7.59	500
4.3	0	-9.60	500
4.4	0	0	500

Tab. 6 Store(s) position; x positive toward leading edge

3. Wing Testing: Numerical and Experimental Investigation

The wing is composed of structural and aerodynamic elements: a Tasmanian oak beam is used as load-carrying element to support the aerodynamic and gravitational loads, while 25 ABS elements provide the aerodynamic shape (NACA 2412 airfoil). This configuration reduces the torsional stiffness of the wing and facilitates the installation of stores between sections at the desired positions. Dynamic tests and modal tests were carried out for the assembled wing with and without stores (see Fig. 14). Selected number and store's positions in spanwise, chordwise, and flapwise direction were considered.

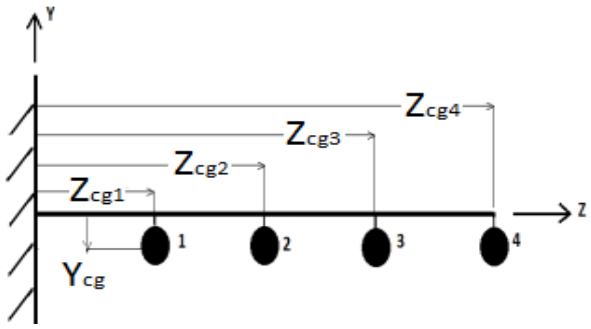

Fig. 14 Position stores numbering.

In Table 6 are reported the positions of the store in each configuration where x, y and z are the CG store positions related to the wing elastic axis. For configuration 4, i.e. when the store is located at the tip, several pod positions in the cross-sectional plane have been investigated: Store CG coincident with the elastic axis (EA) in chord-wise (CW) direction, and positioned 7.59*mm* under the EA

Some configurations are shown in Fig. 15. In this case the wing included 24 ABS parts of 20mm width each, interposing ten additional 2mm segments containing the added stores. This solution was adopted as to not increase the length of the beam. The stores were added to the beam with a 2mm special titanium fastening while. Numerical analysis and experimental campaign were performed taking into account the effect of the nonlinearities. The inertia of the store is comparable with the wing's inertia being the inertia related to the 3 principal directions that are showed in Table 5. Linear/nonlinear numerical and experimental campaigns were performed following the same process described for the individual beam testing. Table 7 through 9 provide the first 6 natural frequencies for selected store positions. When the position of the store moves toward the tip of the wing, the modal characteristics change, indeed the modal shapes and the frequencies are deeply influenced by the concentrated mass movement at different places of the wing. The errors between numerical and experimental predictions are within 5% and it is possible to notice that the torsion experimental frequency is always greater than

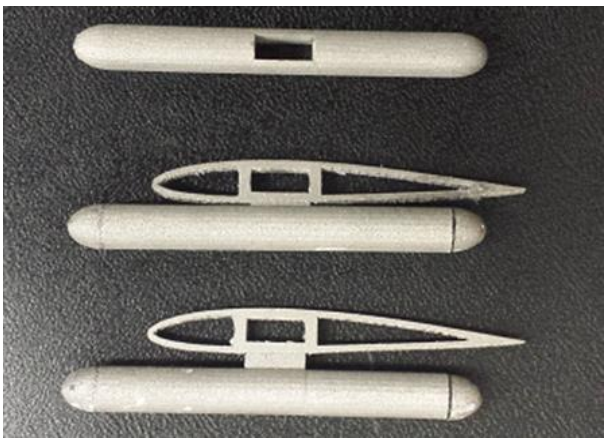

Fig. 15 External shape parts with pods.

	L.N.	L.E.	NL.N.	NL.E
bdg1	4.76	4.88	4.76	4.88
bdg2	28.60	29.30	28.60	29.30
bdg3	65.71	61.36	65.75	65.03
edg1	11.61	11.72	11.56	12.1
edg2	67.38	68.94	67.41	64.45
trs1	24.56	26.17	24.63	25.97

Tab. 7 Position 1 frequencies [Hz]. (L) Linear, (NL) Nonlinear, (N) Numerical, (E) Experimental.

the numerical one. In the numerical model the torsional stiffness was not considered while in the experimental case the torsional stiffness is reduced as minimum as possible but could not be eliminated. When a concentrated mass is applied on the wing the effect of the nonlinearities is reduced, indeed the effect of the nonlinearities on the frequencies is under the 5%. That is because the prevalent effect is the added mass which reduces the frequencies respect to the nonlinear effect due to increased deflection induced by the concentrated mass.

The effect of one single store placed in different span position is reported in Fig. 16. The first frequency of each mode decreases when the pod moves toward the tip position. However, when the pod is placed near the root, the first frequency of each mode is higher than the frequency of the clean wing since there is an increase in stiffness. This effect vanish when the pod move toward the tip, in fact when the pod position reach the 40% of the wing span the effect of the increased mass prevail to the effect of the increased stiffness and the frequencies are lower than in the clean wing case.

The condition 4.1, 4.2, 4.3 are related to the chord-wise pod variation. The 4.1 represents exactly the case related to Tab. 9. The other two cases were related to a forward and backward relative position of the store with respect to the elastic axis, see Fig. 17.

The numerical model predicts the same frequencies for both the linear and the nonlinear case when the CG moves in the chord-wise direction.

The maximum error in the flap-wise and edge-wise bending of about 8% was found for the low frequency and is therefore considered acceptable; however higher error occurred in the high frequency range. The torsion frequencies also present an error, the numerical model underestimate the frequencies in every case. Indeed edge and bending frequencies increase when the pod CG moves from the trailing edge to the leading edge. The reason is the influence of the stores mass that changes the contribution of the inertia which is proportional to the square of the distance. An opposed behaviour was found in the torsion frequencies. This is due to how the torsional frequency are calculated, contrarily to the bending and edge frequencies, it is inversely proportional to the inertia; then when the pod move away from the global CG, the inertia increases, decreasing the associated frequencies.

4. Conclusion

Numerical and experimental investigations to understand the nonlinear effect due to large deformation on the dynamic behaviour of flexible high-aspect ratio wings is considered. The study demonstrates that among others edge and torsion frequencies are the most significantly affected by the large deformed state. That is, for increasing tip displacement, a stronger nonlinear coupling between these

	L.N.	L.E.	NL.N.	NL.E
bdg1	4.32	4.39	4.32	4.28
bdg2	29.65	28.51	29.65	29.3
bdg3	71.70	72.64	71.9	70.01
edg1	10.54	10.55	10.48	10.54
edg2	69.65	66.80	69.53	68.16
trs1	22.36	23.40	22.46	23.01

Tab. 8 Position 3 frequencies [Hz]. (L) Linear, (NL) Nonlinear, (N) Numerical, (E) Experimental.

	L.N.	L.E.	NL.N.	NL.E
bdg1	3.89	4.10	3.89	4.10
bdg2	26.08	26.56	26.08	26.95
bdg3	74.69	71.94	74.66	71.68
edg1	9.49	9.76	9.42	9.76
edg2	60.83	55.50	60.75	57.62
trs1	21.57	21.90	21.675	22.46

Tab. 9 Position 4 frequencies [Hz]. (L) Linear, (NL) Nonlinear, (N) Numerical, (E) Experimental.

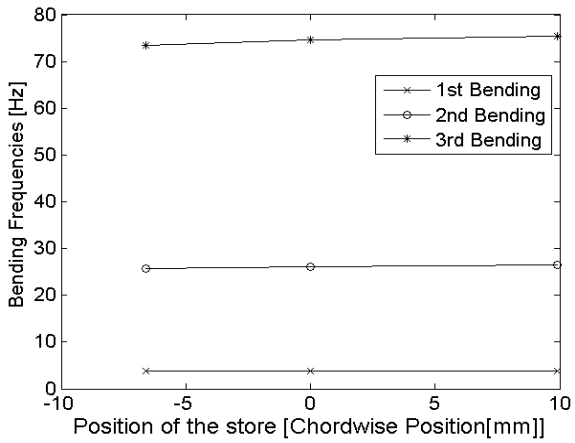

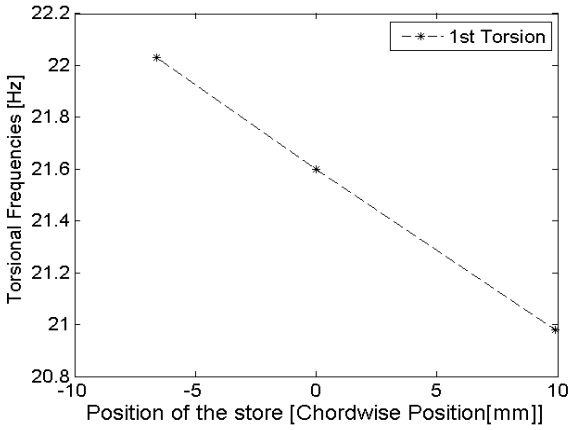

Fig. 17 Effect of the chord wise position; Bending and torsion respectively.

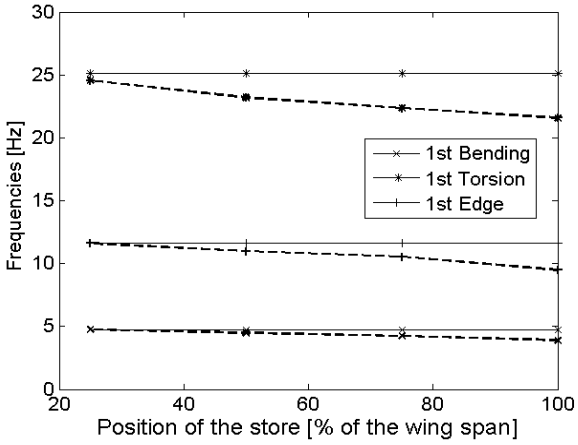

Fig. 16 Store effect in wingspan

frequencies is experienced. The experimental investigations confirmed the numerical predictions. The number and position of stores also strongly affects both frequencies and mode shape. The dynamic response of the structure changes considerably when stores are added, and when stores are moved in the span wise, flap-wise or edge-wise positions. The centre of gravity of the store and his position related to the elastic axis can provide stabilizing, when mode forward the EA, or de-stabilizing when mode backward the EA, contribution on the flap and edge frequencies and the opposite behaviour was found for the torsion frequencies. The model realized for the numerical analysis it is proven to be high fidelity, with a low error related to the experimental data carried out using a laser scan vibrometer with a point load white noise source provided by a shaker.

Bibliography

[1] **E. Cestino, G. Frulla, E. Perrotto and P. Marzocca,** "Experimental slender wing model design by the application of aeroelastic scaling laws", *Journal of Aerospace Engineering*, Vol. 27, No. 1, 2014, pp. 112-120

[2] **E. Cestino, G. Frulla, E. Perrotto and P. Marzocca** "Theoretical and experimental flutter predictions in high aspect ratio composite wings", *SAE International Journal of Aerospace*, Vol. 4, No. 2, 2011, pp. 1365-1372.

[3] **G. Frulla, E. Cestino and P. Marzocca** "Critical behaviour of slender wing configurations", *Part G: Journal of Aerospace Engineering*, Vol. 224, No. 5, 2010, pp. 587-600.

[4]. **M. J. Patil and D. H. Hodges,** "Limit-Cycle oscillations in high-aspect-ratio wings", *Journal of Fluids and Structures*, Vol. 15, No. 1, 2001, pp. 107-132.

[5] **E. Dowell, J. Edwards and T. Strganac** "Nonlinear aeroelasticity", *Journal of Aircraft*, Vol. 40, No. 5, 2003, pp. 857-874.

[6] **K. Abbas, Q. Chen, P. Marzocca and A. Milanese,** "Nonlinear Aeroelastic Investigations of Store(s)-Induced Limit Cycle Oscillation," *Part G: Journal of Aerospace Engineering*, Vol. 222, No. 1, 2008, pp. 63-80.

[7] **M. J. Patil and D. H. Hodges** "On the importance of aerodynamic and structural geometrical nonlinearities in aeroelastic behavior of high-aspect ratio wings", *Journal of Fluids and Structures*, Vol. 19, No. 7, 2004, pp. 905–915.

Copyright Statement